ELSEVIER

www.elsevier.nl/locate/jorganchem

Journal of Organometallic Chemistry 595 (2000) 70–80

Journal of Organometallic Chemistry

Synthesis, electrochemistry and structural characterization of new dimeric cobalt η^2-alkyne carbonyl complexes

Wai-Yeung Wong *, Hoi-Yan Lam, Siu-Ming Lee

Department of Chemistry, Hong Kong Baptist University, Waterloo Road, Kowloon Tong, Hong Kong, People's Republic of China

Received 6 August 1999; received in revised form 17 September 1999

Abstract

New dimeric η^2-diyne complexes of cobalt [$\{Co_2(CO)_6\}_2$(diyne)] (diyne = $Me_3SiC_2(C_{13}H_8)C_2SiMe_3$ (**1**), $Me_3SiC_2(C_{13}H_6O)C_2SiMe_3$ (**2**), $Me_3SiC_2(C_4H_2S)_2C_2SiMe_3$ (**3**), $Me_3SiC_2(C_{14}H_7Fc)C_2SiMe_3$ (Fc = ferrocenyl) (**4**), $HC_2(C_{13}H_8)C_2H$ (**5**), $HC_2(C_{13}H_6O)C_2H$ (**6**), $HC_2(C_4H_2S)_2C_2H$ (**7**) and $HC_2(C_{14}H_7Fc)C_2H$ (**8**)) have been prepared in good yields from the reaction of $[Co_2(CO)_8]$ with half an equivalent of the appropriate diyne ligands $Me_3SiC{\equiv}CRC{\equiv}CSiMe_3$ and $HC{\equiv}CRC{\equiv}CH$, respectively (R = 2,7-fluorenediyl, 2,7-fluoren-9-onediyl, 2,2′-bithiophene-5,5′-diyl, 9-ferrocenylmethylenefluorene-2,7-diyl). All the compounds **1**–**8** have been characterized by IR and ^{1}H-NMR spectroscopies and mass spectrometry. The redox chemistry of these cobalt–alkyne molecules has been studied by cyclic voltammetry. The molecular structures of **2**, **5**, **6**, **7** and **8** have been determined by single-crystal X-ray diffraction methods. Structurally, each of these displays two 'Co_2C_2' cores adopting the usual pseudo-tetrahedral geometry with the alkyne bond lying essentially perpendicular to the Co–Co vector. The original linearity of the diyne ligand is lost.

Keywords: Cobalt; Alkyne; Fluorene; Ferrocenyl; Crystal structures

1. Introduction

Polymers and oligomers containing the acetylide groups are under intensive study because of the possibility of charge transfer along the conjugated backbone and their potential application as building blocks in the design of novel materials [1]. It is well known that the alkyne unit is a versatile functional group, which undergoes a large number of useful transformations [2]. Acetylenes are important precursors for the molecular carbon rod and cyclo[n] species [3]. The use of alkyne complexation to facilitate ring formation is exemplified by the successful isolation of a hexacobalt complex of cyclo[18] carbon from $[Co_2(CO)_6(Me_3SiC_2H)]$ [4] and an octacobalt complex of [8,8]paracyclophaneoctayne [5]. The role of cobalt–alkyne complexes in organic synthesis is also well-established [6].

We are interested in the intramolecular redox chemistry of molecular species with alkyne functionality. Electronic interaction between adjacent organometallic moieties, which are readily oxidized or reduced, can lead to a range of electron-transfer responses [7]. Redox studies on many transition metal carbonyl clusters have demonstrated that they are electron reservoirs with tunable redox behavior dependent on the coordination sphere of the metal framework [7,8]. Such a cluster unit, when incorporated to other redox centers such as ferrocene, can also participate in electronic interactions leading to classical mixed-valence molecules [9]. The $Co_2(CO)_6$ unit is known to coordinate with the C≡C bond in an η^2-fashion [10,11]. Electrochemical study of these compounds suggested that the coordination of the cobalt carbonyl groups maintains the rigidity of the system and still allows for potential electronic delocalization down the chain [11]. The fluorenyl, and oligothienyl derivatives have long been recognized to be important components in semiconductor technology [12]. We believe that the incorporation of $Co_2(CO)_6$ moieties with the acetylide-functionalized fluorene and oligothiophene derivatives would impart interesting properties on the individual molecules. As a continuation of our interest in the chemistry of organometallic polymers, $[-M(L)_xC{\equiv}C-R-C{\equiv}C-]_n$, we describe herein the preparation of a series of organometallic dimers of the form [$\{Co_2(CO)_6\}_2$(diyne)]. The spectroscopic char-

* Corresponding author. Fax: +852-2339-7348.
E-mail address: rwywong@net1.hkbu.edu.hk (W.-Y. Wong)

0022-328X/00/$ - see front matter
PII: S0022-328X(99)00574-4

acterization and electrochemical properties of the complexes are described along with single-crystal X-ray structure analyses of selected complexes.

2. Results and discussion

2.1. Synthesis

The synthesis of all new compounds is outlined in Scheme 1. The organometallic dimers [{$Co_2(CO)_6$}$_2$-(diyne)] (diyne = $Me_3SiC_2(C_{13}H_8)C_2SiMe_3$ (**1**), Me_3SiC_2-$(C_{13}H_6O)C_2SiMe_3$ (**2**), $Me_3SiC_2(C_4H_2S)_2C_2SiMe_3$ (**3**), $Me_3SiC_2(C_{14}H_7Fc)C_2SiMe_3$ (Fc = ferrocenyl) (**4**), HC_2-$(C_{13}H_8)C_2H$ (**5**), $HC_2(C_{13}H_6O)C_2H$ (**6**), $HC_2(C_4H_2S)_2$-C_2H (**7**) and $HC_2(C_{14}H_7Fc)C_2H$ (**8**)) were prepared from the reactions of two molar equivalents of octacarbonyldicobalt(0), [$Co_2(CO)_8$], with the appropriate diynes in *n*-hexane at 0°C. The ligands used embrace 2,7-bis(trimethylsilylethynyl)fluorene, 2,7-bis(trimethylsilylethynyl)fluoren-9-one, 5,5′-bis(trimethylsilylethynyl)-2,2′-bithiophene, 9-ferrocenylmethylene-2,7-bis(trimethylsilylethynyl)fluorene, 2,7-diethynylfluorene, 2,7-diethynylfluoren-9-one, 5,5′-diethynyl-2,2′-bithiophene and 9-ferrocenylmethylene-2,7-diethynylfluorene [12]. The reactions were readily monitored by thin-layer chromatography (TLC) and solution IR spectroscopy in the 2200–1600 cm^{-1} region. Purification of the crude products was accomplished by preparative TLC on silica using hexane as eluent to afford dark-red microcrystalline solids after recrystallization. The dimeric compounds are soluble in common organic solvents. In all cases, the products are not air-sensitive in the solid form but slowly decompose to uncharacterized black materials in solution in several days. The formulae of these complexes were first established by positive fast atom bombardment (FAB) mass spectrometry and IR and ^{1}H-NMR spectroscopies, and they all gave satisfactory microanalytical data.

2.2. Spectroscopic characterization

Table 1 summarizes basic spectroscopic data for all the new compounds in this study. The IR spectra in the carbonyl region for complexes **1**–**8** show signals corresponding to terminal carbonyl ligands only. These spectral patterns are similar to those observed for previously reported cobalt–alkyne complexes [10,13]. The bridging carbonyl bands due to the parent [$Co_2(CO)_8$] are completely absent. The absence of ν(C≡C) in the region of 2100 cm^{-1} (for **1**–**8**) and ν(C≡CH) around 3300 cm^{-1} (for **5**–**8**) indicates that the alkynyl bond loses its triple-bond character and

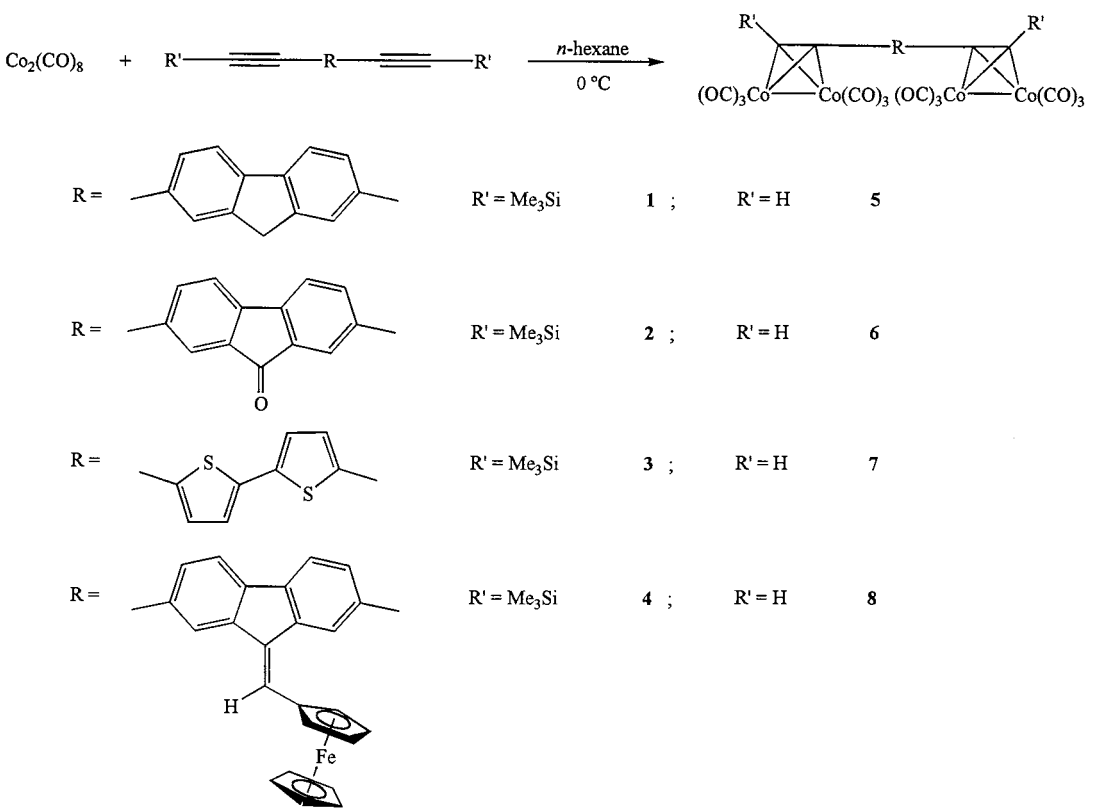

Scheme 1.

Table 1
Spectroscopic data for complexes **1**–**8**

Complex	IR (cm^{-1}) [a]	^{1}H-NMR (δ, J/Hz) [b]	FAB MS (m/z) [c]
1	2086m, 2052vs, 2024vs, 2008sh	0.42 (s, 18H, $SiMe_3$) 3.91 (s, 2H, CH_2) 7.55 (br, 2H, aromatic CH) 7.66 (m, 2H, aromatic CH) 7.71 (d, 2H, J_{H-H} = 7.0, aromatic CH)	902 (930) [d]
2	2088m, 2054vs, 2028vs, 2012sh	0.41 (s, 18H, $SiMe_3$) 7.50 (d, 2H, J_{H-H} = 7.8, aromatic CH) 7.65 (dd, 2H, J_{H-H} = 1.4, 7.8, aromatic CH) 7.72 (d, 2H, J_{H-H} = 1.4, aromatic CH)	916 (944) [d]
3	2088m, 2054vs, 2027s, 2012vw	0.40 (s, 18H, $SiMe_3$) 7.05 (d, 2H, J_{H-H} = 4.0, thienyl CH) 7.15 (d, 2H, J_{H-H} = 4.0, thienyl CH)	874 (930) [e]
4	2084m, 2049vs, 2019s	0.35 (s, 9H, $SiMe_3$) 0.50 (s, 9H, $SiMe_3$) 4.20 (s, 5H, C_5H_5) 4.48 (t, 2H, C_5H_4) 4.78 (t, 2H, C_5H_4) 7.53 (dd, 1H, J_{H-H} = 1.6, 7.8, aromatic CH) 7.56 (dd, 1H, J_{H-H} = 1.6, 7.8, aromatic CH) 7.57 (s, 1H, vinyl CH) 7.70 (d, 1H, J_{H-H} = 8.0, aromatic CH) 7.72 (d, 1H, J_{H-H} = 8.0, aromatic CH) 8.00 (d, 1H, J_{H-H} = 8.0, aromatic CH) 8.30 (d, 1H, J_{H-H} = 8.0, aromatic CH)	1126 (1126)
5	2092m, 2058vs, 2029vs, 2014w	3.94 (s, 2H, CH_2) 6.41 (s, 2H, C≡CH) 7.55 (dd, 2H, J_{H-H} = 1.4, 7.8, aromatic CH) 7.67 (d, 2H, J_{H-H} = 1.4, aromatic CH) 7.70 (d, 2H, J_{H-H} = 7.8, aromatic CH)	786 (786)
6	2092m, 2057vs, 2028s	6.40 (s, 2H, C≡CH) 7.51 (d, 2H, J_{H-H} = 7.7, aromatic CH) 7.68 (dd, 2H, J_{H-H} = 1.3, 7.7, aromatic CH) 7.77 (d, 2H, J_{H-H} = 1.3, aromatic CH)	801 (801)
7	2092w, 2060vs, 2032s, 2018vw	6.30 (s, 2H, C≡CH) 7.04 (d, 2H, J_{H-H} = 4.0, thienyl CH) 7.15 (d, 2H, J_{H-H} = 4.0, thienyl CH)	785 (785)
8	2090m, 2054vs, 2024s	4.14 (s, 5H, C_5H_5) 4.42 (t, 2H, C_5H_4) 4.66 (t, 2H, C_5H_4) 6.29 (s, 1H, C≡CH) 6.43 (s, 1H, C≡CH) 7.43 (dd, 1H, J_{H-H} = 1.3, 7.5, aromatic CH) 7.47 (s, 1H, vinyl CH) 7.49 (dd, 1H, J_{H-H} = 1.3, 7.5, aromatic CH) 7.61 (d, 2H, J_{H-H} = 7.5, aromatic CH) 7.85 (m, 1H, aromatic CH) 8.25 (m, 1H, aromatic CH)	982 (982)

[a] Recorded in CH_2Cl_2.
[b] Recorded in $CDCl_3$.
[c] Calculated values in parentheses.
[d] Only $[M–CO]^+$ is observed.
[e] Only $[M–2CO]^+$ is observed.

both alkyne linkages are coordinated to $Co_2(CO)_6$ units.

The ^{1}H-NMR data for complexes **1**–**8** are consistent with their formulation. The set of proton NMR signals in the range δ 7.0–8.5 evidences the presence of aromatic rings in each case. For the fluorene-containing compounds **1** and **5**, proton resonances arising from the CH_2 unit appear at about δ 3.90. Apart from the features attributed to the aromatic group, complexes **4** and **8** also clearly display two triplets and a singlet in their proton NMR spectra, characteristic for monosubstituted ferrocenyl moieties. The vinyl protons for **4** and

8 resonate in the range δ 7.47–7.67, which integrate as one proton. As expected, the chemical shifts for the Me_3Si and terminal protons are found to be very sensitive to cobalt complexation on the adjacent alkyne bond. For the Me_3Si-substituted complexes **1**–**4**, a single resonance is observed in the range δ 0.35–0.50. Complexes **5**–**8**, which bear a terminal alkyne proton, show a singlet signal in the region δ 6.29–6.43. By comparison with the ^{1}H-NMR spectral data of the free ligands [12], we observe a significant downfield shift for the Me_3Si and C≡CH protons in the Co_2-functionalized complexes by ca. 0.2 and 3 ppm, respectively. Because of the reduction in the triple-bond character upon coordination of $Co_2(CO)_6$, there is a deshielding effect on the adjacent silyl and terminal protons [14].

Most of our compounds gave satisfactory mass spectral data. For complexes **4**–**8**, the positive FAB mass spectra showed the respective molecular ions, as well as peaks corresponding to the consecutive loss of the 12 carbonyl ligands. This is consistent with the fact that two $\{Co_2(CO)_6\}$ moieties have coordinated to the diyne. The FAB mass spectrum of **1** did not show the respective molecular ion, however a peak was observed at m/z 902 corresponding to the molecular ion accompanied by a loss of one carbonyl ligand. For complexes **2** and **3**, peaks at m/z 916 and 874 were observed which corresponded to the molecular fragment $[M-2CO]^+$.

2.3. Electrochemistry

An electrochemical approach has widely been adopted to study the electronic interactions between redox centers in π-conjugated organometallic dimers [15]. A simple criterion is employed for an approximate evaluation of such interactions, i.e. clusters that are interacting in an electrochemical sense would display two reversible couples with a potential separation determined by the extent of the interaction [15]. As such, the redox properties of complexes **1**–**4** were investigated in CH_2Cl_2 at room temperature (r.t.) and at −78°C using cyclic voltammetry with $[NBu_4]PF_6$ as the supporting electrolyte. Redox potential values obtained in this study are given in Table 2.

Table 2
Electrochemical data for complexes **1**–**4** in CH_2Cl_2 [a,b]

Complex	Room temperature	−78°C
1	−1.65 [c], 0.77 [c]	−2.04 (95), −1.57 (80), 0.66 (200)
2	−1.57 [c], 0.88 [c]	−1.75 (85), −1.52 (80), 0.75 (200)
3	−1.58 [c], 0.62 [c]	−2.01 (100), −1.58 (91), 0.71 (200)
4	−1.56 [c], 0.23 (87), 0.78 [c]	−2.08 (100), −1.57 (100), 0.23 (87), 0.69 (150)

[a] The electrochemical measurements were made at a glassy-carbon working electrode containing 0.1 M $[NBu_4]PF_6$ as base electrolyte, using a scan rate of 100 mV s^{-1}. All potentials were quoted in volts versus the ferrocene/ferrocenium couple that was used as an internal standard.

[b] The difference between the anodic and cathodic peak potentials for a reversible wave is shown in parentheses.

[c] Irreversible wave.

The $Co_2(CO)_6$ entity bound to an alkyne was reported by Robinson and co-workers to undergo an irreversible reduction at potentials in the range −0.65 to −1.10 V versus Ag/AgCl in CH_2Cl_2 at r.t. [16]. We observed this expected reduction at potentials ranging from −1.56 to −1.65 V versus ferrocene/ferrocenium (Fc/Fc^+) couple in CH_2Cl_2 at r.t. for complexes **1**–**4**, which is believed to be cobalt cluster based. At ambient temperature, each of the complexes **1**–**4** undergoes an irreversible reduction process followed by an oxidation event in the potential range 0.62–0.88 V due to $[Co(CO)_4]^-$ resulting from the decomposition of the electrogenerated monoanion [15,16]. At first sight, one might be tempted to think that there is no electrochemically detectable electronic communication between the Co_2 cores. In fact, it has been shown that the fast chemical decomposition following the redox process in all these compounds prevents proper electrochemical analysis.

With an attempt to resolve the problem, voltammetric measurements were carried out at a lower temperature. At −78°C complications were completely quenched so that chemical reversibility was achieved. The reduction waves for **1**–**4** gradually split into two apparently chemically reversible one-electron transfer peaks, with a splitting of 470 mV for **1**, 230 mV for **2**, 430 mV for **3** and 510 mV for **4**. Such an observation suggests that, despite the two redox centers being identical, they are coupled from an electronic perspective. These values may be compared with the smaller splitting of 220 mV found in $[\{Co_2(CO)_6\}_2(PhC{\equiv}C{-}C{\equiv}CPh)]$ [15] and this indicates that the presence of aromatic entities within the diyne ligands tends to increase the electronic communication between the two Co_2 moieties. Moreover, it is interesting to note that attachment of an electron-donating ferrocenyl group contributes to the largest splitting as in **4**, whereas the smallest peak separation in **2** is achieved with an electron-withdrawing fluorenone moiety. It is therefore envisaged that the coupling between the redox centers can be modulated by modification of the donor–acceptor characteristics of the central linkers.

The ferrocenyl residue in **4** is characterized by a reversible one-electron oxidation wave at 0.23 V versus the Fc/Fc^+ couple in CH_2Cl_2. When compared with the free diyne complex, this wave is anodically shifted by ca. 90 mV. The shift is ascribed to conjugation of the ferrocenyl group to the electron-withdrawing $Co_2(CO)_6$ unit via the fluorene bridge, which makes the removal of the electron from the ferrocene core more difficult.

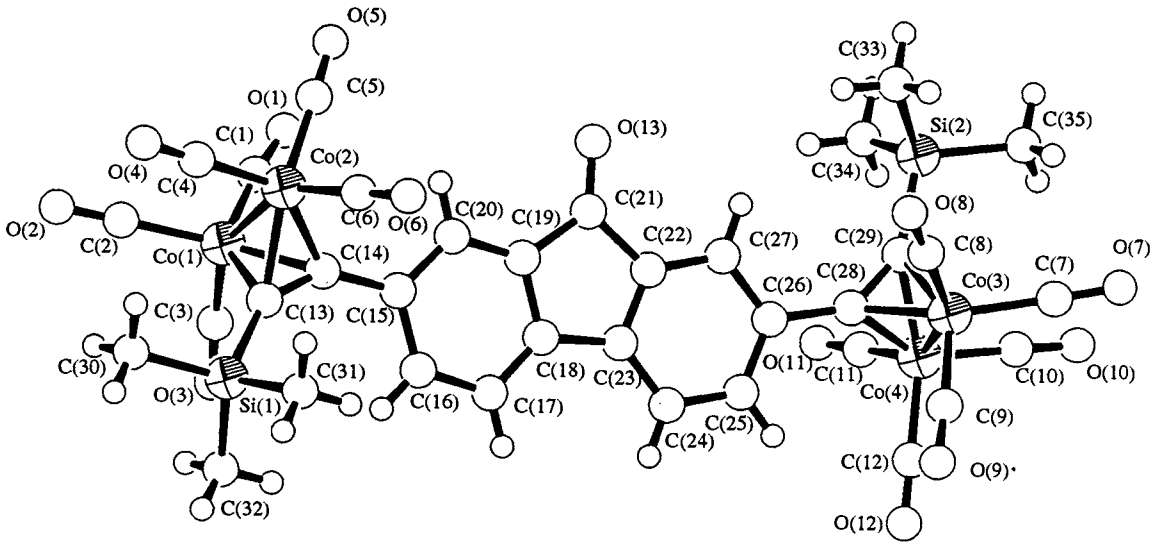

Fig. 1. Molecular structure of **2**, showing the atomic labeling scheme. Co(1)–Co(2), 2.463(3); Co(3)–Co(4), 2.473(3); Co(1)–C(13), 2.00(1); Co(1)–C(14), 1.95 (1); Co(2)–C(13), 2.00(1); Co(2)–C(14), 1.95(1); Co(3)–C(28), 1.96(1); Co(3)–C(29), 1.98(1); Co(4)–C(28), 1.96(1); Co(4)–C(29), 1.98(1); C(13)–C(14), 1.33 (1); C(28)–C(29), 1.33(1); Si(1)–C(13), 1.84(1); Si(2)–C(29), 1.85(1); C(21)–O(13), 1.20(1) Å; Co(2)–Co(1)–C(13), 52.0(3);Co(2)–Co(1)–C(14), 50.9(3); C(13)–Co(1)–C(14), 39.3(4); Co(1)–Co(2)–C(13), 51.9(4); Co(1)–Co(2)–C(14), 50.9(4); C(13)–Co(2)–C(14), 39.2(4); Co(1)–C(13)–C(14), 68.5(8); Co(2)–C(13)–C(14), 68.5(7); Co(1)–C(14)–C(15), 130.6(9); Co(2)–C(14)–C(15), 134.6(9); Co(4)–Co(3)–C(28), 50.7(3); Co(4)–Co(3)–C(29), 51.4(3); C(28)–Co(3)–C(29), 39.5(4); C(28)–Co(4)–C(29), 39.6(4); Co(3)–Co(4)–C(28), 50.9(4); Co(3)–Co(4)–C(29), 51.4(3); Co(3)–C(28)–C(29), 71.1(8); Co(4)–C(28)–C(29), 71.3(7); Co(3)–C(28)–C(26), 130.9(9); Co(4)–C(28)–C(26), 135.1(9); C(13)–C(14)–C(15), 142(1); C(26)–C(28)–C(29), 142(1); Si(1)–C(13)–C(14), 149.4(9); Si(2)–C(29)–C(28), 150(1)°.

2.4. Crystal structure analyses

The solid-state structures of complexes **2**, **5**, **6**, **7** and **8** have successfully been established by X-ray crystallography in order to investigate the effect of complexation on the linearity and rigidity of the diyne system. The crystal structure of **2** consists of discrete molecules of $[\{Co_2(CO)_6\}_2\{Me_3SiC_2(C_{13}H_6O)C_2SiMe_3\}]$, in which the two $Co_2(CO)_6$(alkyne) fragments are linked by the 2,7-fluoren-9-onediyl group. The molecules are separated by the normal van der Waals distance. A perspective view of the molecular structure of **2** is shown in Fig. 1, together with the atomic numbering scheme. The X-ray structure of **2** shows that the two Co_2C_2 cores adopt the usual pseudo-tetrahedral geometry with the alkyne C≡C vector lying essentially perpendicular to the Co–Co vector. Each of the cobalt atoms is coordinated to three terminal carbonyl ligands which exhibit linear geometries. The Co–Co separation (average 2.468 Å) found in **2** is in the region expected for other dicobalt systems that are bridged by perpendicular alkyne ligands, indicating the presence of a metal–metal bond [13,17]. However, such a distance is shorter than that in the parent carbonyl, $[Co_2(CO)_8]$ (average 2.52 Å). A salient structural feature of the structure of **2** is the asymmetry of the Co–C distances in the Co_2C_2 cores. These distances may be divided into two groups, with the average Co–C(13) distance (2.00(1) Å) being ca. 0.05 Å longer than the average Co–C(14) distance (1.95(1) Å). Similar to $[\{Co_2(CO)_6\}_2(Me_3SiC_2C_6H_4C_6H_4C_2SiMe_3)]$ reported previously by Lewis et al. [13], the longer Co–C(alkyne) distances are associated with the carbon coordinated to the $SiMe_3$ group, on the basis of the steric requirements of the $SiMe_3$ unit. With regards to the diyne functionality, the original linearity is found to be lost. Each of the C≡C bond lengths (C(13)–C(14)≡C(28)–C(29) 1.33(1) Å) is lengthened owing to the loss of triple-bond character upon complexation. The bond angles Si(1)–C(13)–C(14), 149.4(9)° and C(13)–C(14)–C(15), 142(1)°, are significantly reduced from the 180° expected for a linear alkyne, consistent with rehybridization of both C(13) and C(14) towards sp^2. The corresponding values for the other Co_2C_2 core are Si(2)–C(29)–C(28), 150(1)° and C(26)–C(28)–C(29), 142(1)°. The central fluorenone group, which is essentially coplanar, is coordinated to one of the alkylenic carbon atoms, C(14) and C(28) and shows a small twist with respect to the alkylenic C–C vector (C(13)–C(14)–C(15)–C(16) 21(2)°, C(13)–C(14)–C(15)–C(20) −161(1)°; C(25)–C(26)–C(28)–C(29) 169(1)°, C(27)–C(26)–C(28)–C(29) −18(2)°).

Fig. 2 depicts the molecular structure of **5**. The basic structural skeleton resembles that of **2** and other dimeric cobalt–alkyne complexes with the two Co_2C_2 units linked through a 2,7-fluorenediyl moiety. In each Co_2C_2 core, the alkyne C≡C vector is perpendicular to the Co–Co vector. The mean Co–Co bond length (2.474(1) Å) is typical of other related dicobalt systems

[13,17]. The alkylenic C–C distance (average 1.334(8) Å] shows a lengthening of ca. 0.15 Å from the value of 1.18 Å found in the free alkyne and 2,7-bis(trimethylsilylethynyl)fluorene [12], an observation that is consistent with a reduction in triple-bond character. Adding to this, the 'bent-back' angles of the fragments C(13)–C(14)–C(15) and C(21)–C(22)–C(23) are 37.2(6) and 37.8(6)°, respectively. An analysis of the four Co–C(alkyne) distances in **5** shows that they can again be grouped into two sets. The two Co–C(13) distances average ca. 1.949(7) Å, whereas the bonds Co–C(14) are longer, with an average distance of 1.977(6) Å. Therefore, the Co_2C_2 pseudo-tetrahedron is distorted with the longer Co–C(alkyne) interactions being associated with the alkylenic carbon coordinated to the central fluorene ring. This feature is in contrast with that observed for **2**.

A perspective drawing of compound **6** is shown in Fig. 3, along with the atom-numbering scheme. The overall structure resembles those of compounds **2** and **5**

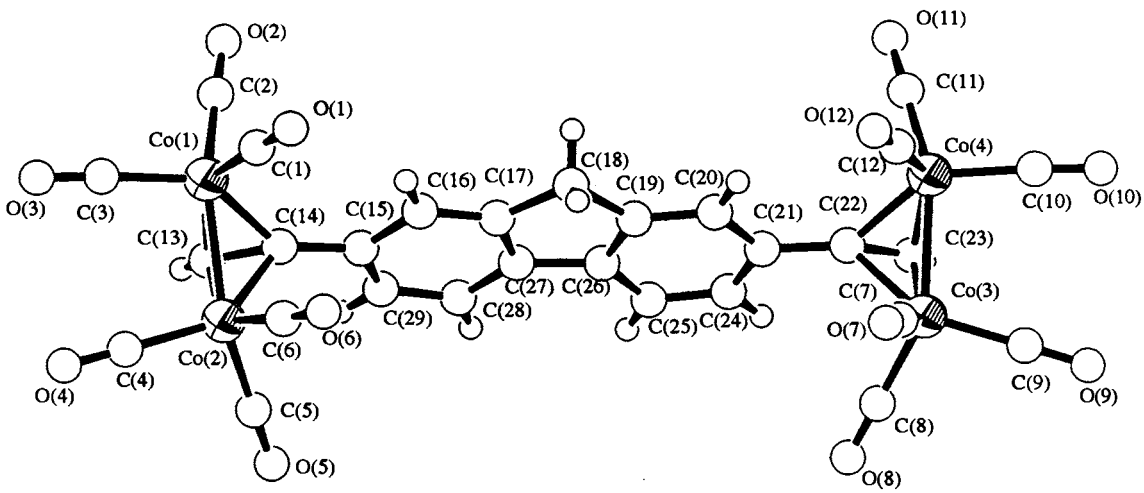

Fig. 2. Molecular structure of **5**, showing the atomic labeling scheme. Co(1)–Co(2), 2.473(1); Co(3)–Co(4), 2.475(1); Co(1)–C(13), 1.954(6); Co(1)–C(14), 1.954 (6); Co(2)–C(13), 1.943(7); Co(2)–C(14), 1.999(6); Co(3)–C(22), 1.999(6); Co(3)–C(23), 1.937(7); Co(4)–C(22), 1.962(6); Co(4)–C(23), 1.950(6); C(13)–C(14), 1.334(8); C(22)–C(23), 1.333(8) Å; Co(2)–Co(1)–C(13), 50.4(2); Co(2)–Co(1)–C(14), 52.1(2); C(13)–Co(1)–C(14), 39.9(2); Co(1)–Co(2)–C(13), 50.8(2); Co(1)–Co(2)–C(14), 50.5(2); C(13)–Co(2)–C(14), 39.5(2); Co(1)–C(13)–C(14), 70.1(4); Co(2)–C(13)–C(14), 72.5(4); Co(1)–C(14)–C(15), 140.0(4); Co(2)–C(14)–C(15), 128.6(5); Co(4)–Co(3)–C(22), 50.7(2); Co(4)–Co(3)–C(23), 50.7(2); C(22)–Co(3)–C(23), 39.5(2); C(22)–Co(4)–C(23), 39.8(2); Co(3)–Co(4)–C(22), 52.0(2); Co(3)–Co(4)–C(23), 50.2(2); Co(3)–C(22)–C(23), 67.7(4); Co(4)–C(22)–C(23), 69.6(3); Co(3)–C(22)–C(21), 130.8(5); Co(4)–C(22)–C(21), 139.3(5); C(13)–C(14)–C(15), 142.8(6); C(21)–C(22)–C(23), 142.2(6)°.

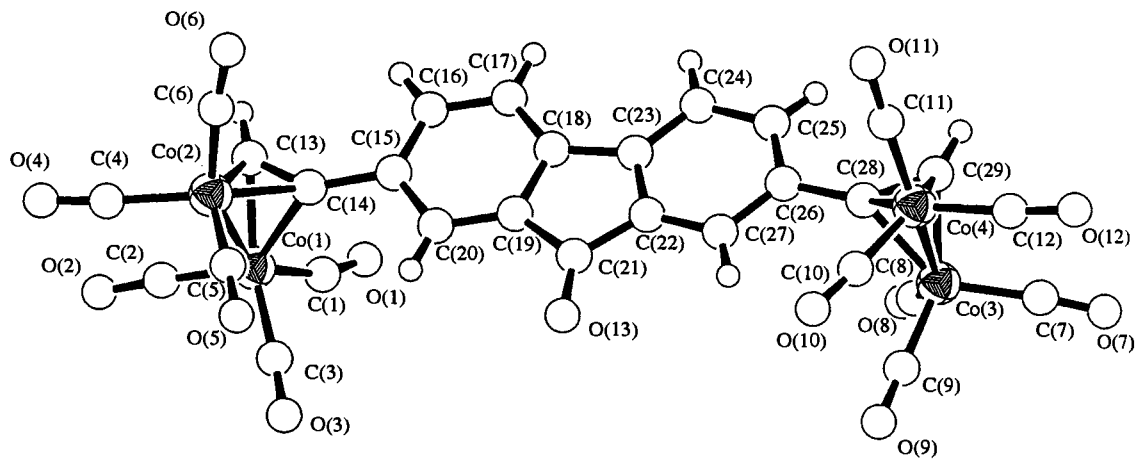

Fig. 3. Molecular structure of **6**, showing the atomic labeling scheme. Co(1)–Co(2), 2.461(3); Co(3)–Co(4), 2.470(3); Co(1)–C(13), 1.91(1); Co(1)–C(14), 1.97(1); Co(2)–C(13), 1.89(1); Co(2)–C(14), 1.96(1); Co(3)–C(28), 1.98(1); Co(3)–C(29), 1.91(1); Co(4)–C(28), 1.96(1); Co(4)–C(29), 1.92(1); C(13)–C(14), 1.32(1); C(28)–C(29), 1.33(2); C(21)–O(13), 1.20(1) Å; Co(2)–Co(1)–C(13), 49.4(4); Co(2)–Co(1)–C(14), 51.1(4); C(13)–Co(1)–C(14), 39.6(4); Co(1)–Co(2)–C(13), 50.1(4); Co(1)–Co(2)–C(14), 51.3(3); C(13)–Co(2)–C(14), 39.9(5); Co(1)–C(13)–C(14), 72.4(8); Co(2)–C(13)–C(14), 72.8(8); Co(1)–C(14)–C(15), 133.2(8); Co(2)–C(14)–C(15), 139.0(8); Co(4)–Co(3)–C(28), 50.7(4); Co(4)–Co(3)–C(29), 50.2(4); C(28)–Co(3)–C(29), 40.1(5); C(28)–Co(4)–C(29), 40.2(5); Co(3)–Co(4)–C(28), 51.5(4); Co(3)–Co(4)–C(29), 49.6(4); Co(3)–C(28)–C(29), 67.2(8); Co(4)–C(28)–C(29), 68.6(8); Co(3)–C(28)–C(26), 134(1); Co(4)–C(28)–C(26), 137(1); C(13)–C(14)–C(15), 141(1); C(26)–C(28)–C(29), 141(1)°.

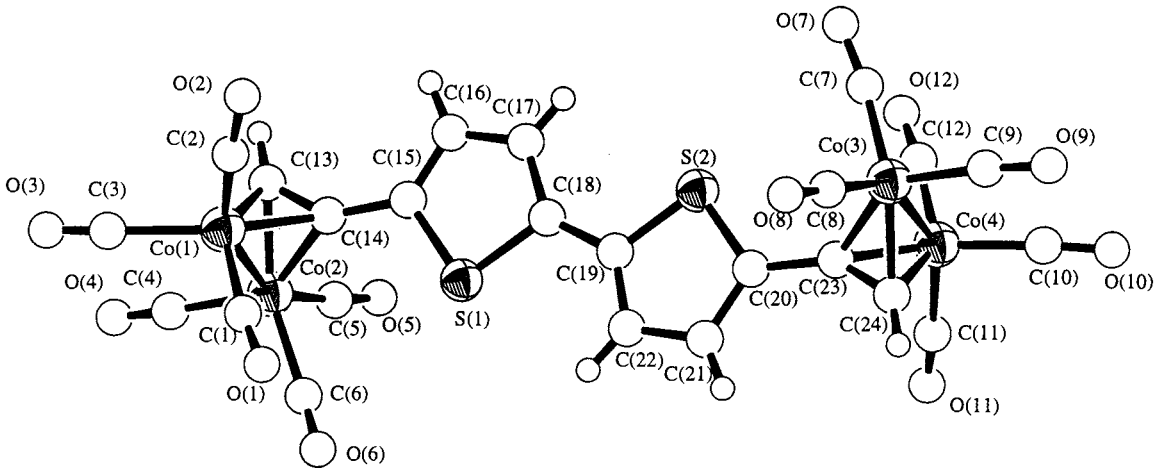

Fig. 4. Molecular structure of **7**, showing the atomic labeling scheme. Co(1)–Co(2), 2.465(5); Co(3)–Co(4), 2.484(6); Co(1)–C(13), 1.88(3); Co(1)–C(14), 1.97(2); Co(2)–C(13), 1.94(3); Co(2)–C(14), 1.95(2); Co(3)–C(23), 1.93(2); Co(3)–C(24), 1.91(3); Co(4)–C(23), 1.96(2); Co(4)–C(24), 1.96(3); C(13)–C(14), 1.29(4); C(23)–C(24), 1.28(3) Å; Co(2)–Co(1)–C(13), 50.8(9); Co(2)–Co(1)–C(14), 50.7(7); C(13)–Co(1)–C(14), 39(1); Co(1)–Co(2)–C(13), 48.8(8); Co(1)–Co(2)–C(14), 51.5(7); C(13)–Co(2)–C(14), 38(1); Co(1)–C(13)–C(14), 74(1); Co(2)–C(13)–C(14), 71(1); Co(1)–C(14)–C(15), 133(1); Co(2)–C(14)–C(15), 137(1); Co(4)–Co(3)–C(23), 50.8(7); Co(4)–Co(3)–C(24), 50.8(8); C(23)–Co(3)–C(24), 39(1); C(23)–Co(4)–C(24), 38(1); Co(3)–Co(4)–C(23), 49.8(7); Co(3)–Co(4)–C(24), 49.1(8); Co(3)–C(23)–C(24), 69(1); Co(4)–C(23)–C(24), 70(1); Co(3)–C(23)–C(20), 134(1); Co(4)–C(23)–C(20), 132(1); C(13)–C(14)–C(15), 141(2); C(20)–C(23)–C(24), 143(2)°.

mentioned above. Analogous to **5** with terminal protons on the alkyne C≡C bond, an asymmetry of Co–C distances is also observed in **6** with a difference of ca. 0.07 Å. The alkylenic C≡C bond lengths (1.32(1)–1.33(2) Å) also lie within the expected range for alkyne groups bound to $Co_2(CO)_6$ units and bending of the initially linear alkyne bond is apparent.

The molecular structure of **7** is illustrated in Fig. 4. The crystal structure consists of discrete dimeric molecules in which the $Co_2(CO)_6$ units are coordinated to the C≡C bonds of 5,5′-diethynyl-2,2′-bithiophene in an η^2-mode forming distorted pseudo-Co_2C_2 tetrahedra. As in the structure of 5,5′-bis(trimethylsilylethynyl)-2,2′-bithiophene and *trans*-[$(Et_3P)_2PhPt$–C≡CRC≡C–$PtPh(PEt_3)_2$] (R = bithiophenediyl) [12], the two thiophene rings in **7** display a *trans* arrangement in order to minimize the steric repulsions between the lone pairs on both sulfur atoms. The C–C bond distances of the thiophene ring span from 1.33(3) to 1.44(4) Å with an average of 1.38(4) Å. This average is the same as that observed in 5,5′-bis(trimethylsilylethynyl)-2,2′-bithiophene [12]. Slight shortening of the bonds C(14)–C(15) and C(18)–C(19) (1.43(3) and 1.41(3) Å, respectively) is consistent with a partial π component. The remaining interatomic distances and angles in the molecule are normal and compare well with the values reported above.

The molecular structure of the ferrocenylfluorene derivative **8**, as determined crystallographically, is depicted in Fig. 5, which includes the atom numbering scheme. Structurally, the molecule comprises a ferrocene entity appended to the ferrocenyl moiety at the 9 position via C(30) atom (C(25)–C(30) 1.34(2) Å) and two '$Co_2(CO)_6C_2$' units are coordinated to the ferrocenylfluorene group at the 2,7 positions. As far as the comformation of the cyclopentadienyl rings of the ferrocenyl group is concerned, the staggered nature of the rings is confirmed by the X-ray structural determination with a deviation of 32.2°. The two Cp rings are almost planar and they are nearly parallel, with a very small ring tilt angle (2.0°). The fluorenyl ring system makes a dihedral angle of 42.3° with the monosubstituted η^5-C_5H_4 ring.

3. Conclusions

A series of $Co_2(CO)_6$-coordinated diyne complexes have been prepared and, in most cases, structurally characterized by X-ray crystallography. These new compounds are electrochemically active and low-temperature cyclic voltammetric responses display two well-resolved chemically reversible one-electron couples. The most significant electrochemical fact is that the two $Co_2(CO)_6$ redox centers are electronically coupled, although they are identical. Homonuclear organometallic clusters of the type discussed in this paper have provided an important class of compounds to evaluate the extent to which intramolecular electronic interactions can be modulated by the electronic characteristics of the linkage between the metal units. It is clear that there is a significant difference in the redox potentials and splitting parameters (470 mV **1**, 230 mV **2**, 430 mV **3** and 510 mV **4**) with varying spacer groups between $Co_2(CO)_6$ moieties. For the heterometallic (Co–Fe–Co)

complex **4**, the splitting is the largest with the introduction of an electron-donating ferrocenyl group and the Fc/Fc^+ couple is also found to be anodically shifted as compared to the free ligand precursor.

4. Experimental

4.1. General procedures

All operations were carried out under an atmosphere of dinitrogen using standard Schlenk techniques, but no special precautions were taken to exclude oxygen during work-up. All chemicals, unless otherwise stated, were from commercial sources and used as received. The compounds 2,7-bis(trimethylsilylethynyl)fluorene, 2,7-diethynylfluorene, 2,7-bis(trimethylsilylethynyl) fluoren-9-one, 2,7-diethynylfluoren-9-one, 5,5′-bis-(trimethylsilylethynyl)-2,2′-bithiophene, 5,5′-diethynyl-2,2′-bithiophene, 9-ferrocenylmethylene-2,7-bis(trimethylsilylethynyl)fluorene and 9-ferrocenylmethylene-2,7-diethynylfluorene were prepared according to the published methods [12]. Solvents were predried and distilled from appropriate drying agents [18]. Infrared spectra were recorded as CH_2Cl_2 solutions in a CaF_2 cell (0.5 mm path length), on a Perkin–Elmer Paragon 1000 FTIR spectrometer. Proton NMR spectra were recorded in $CDCl_3$ on a Jeol GX270 FT NMR spectrometer. Chemical shifts were quoted relative to $SiMe_4$ ($\delta = 0$). FAB mass spectra were recorded on a Finnigan MAT 95 mass spectrometer. Electrochemical measurements were made using a PC-controlled EG&G-PAR 273A potentiostat. A conventional three-electrode cell was used, with a glassy-carbon working electrode, a Pt-wire counter electrode and a $Ag/AgNO_3$ reference electrode. Ferrocene was added as a calibrant after each set of measurements and all potentials were quoted relative to the ferrocene–ferrocenium couple (taken as $E_{1/2} = 0.220$ V in CH_2Cl_2). Preparative TLC was carried out on 0.7 mm silica plates (Merck Kieselgel 60 GF_{254}) prepared in this laboratory.

4.2. Preparations of complexes *1*–*8*

All the cobalt–alkyne complexes **1**–**8** in this study were synthesized by following a general procedure outlined below for **1**.

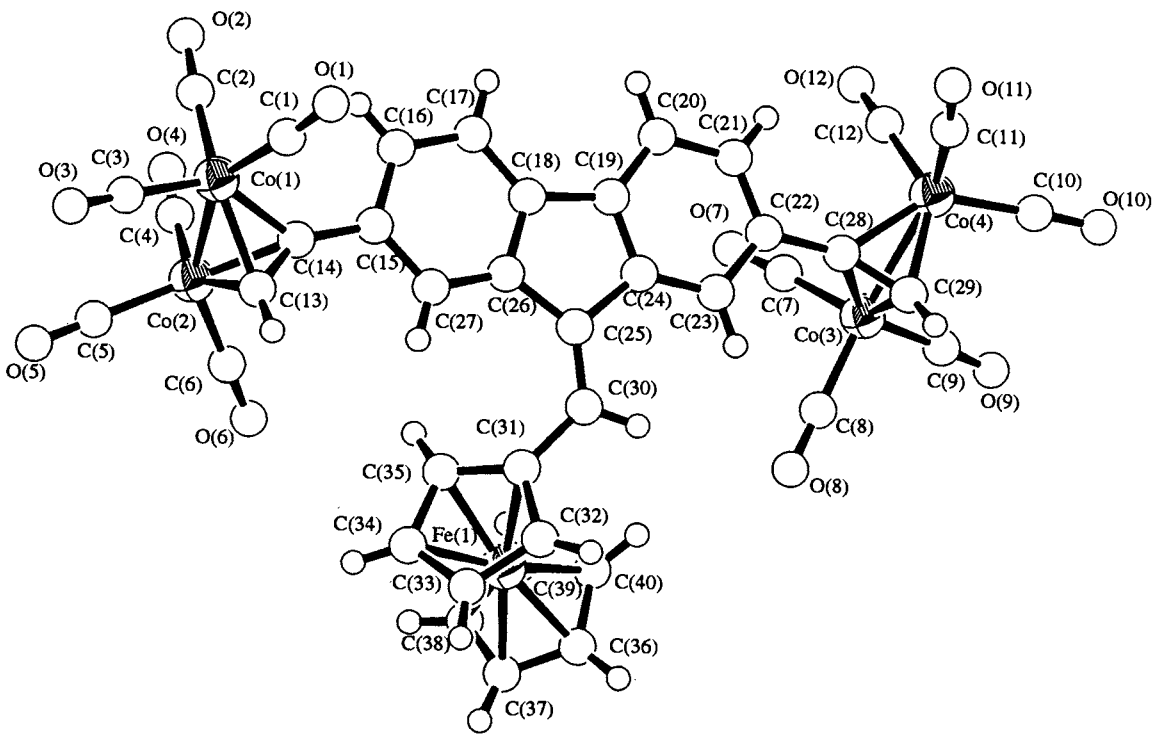

Fig. 5. Molecular structure of **8**, showing the atomic labeling scheme. Co(1)–Co(2), 2.470(4); Co(3)–Co(4), 2.482(4); Co(1)–C(13), 1.96(2); Co(1)–C(14), 1.93(1); Co(2)–C(13), 1.90(2); Co(2)–C(14), 1.98(1); Co(3)–C(28), 2.00(2); Co(3)–C(29), 1.93(2); Co(4)–C(28), 1.96(1); Co(4)–C(29), 1.95(1); C(13)–C(14), 1.31(2); C(28)–C(29), 1.31(2); C(25)–C(30), 1.34(2); C(30)–C(31), 1.48(2) Å; Co(2)–Co(1)–C(13), 49.3(5); Co(2)–Co(1)–C(14), 51.8(4); C(13)–Co(1)–C(14), 39.3(5); Co(1)–Co(2)–C(13), 51.3(5); Co(1)–Co(2)–C(14), 50.1(4); C(13)–Co(2)–C(14), 39.3(5); Co(1)–C(13)–C(14), 69(1); Co(2)–C(13)–C(14), 74(1); Co(1)–C(14)–C(15), 136(1); Co(2)–C(14)–C(15), 131(1); Co(4)–Co(3)–C(28), 50.5(4); Co(4)–Co(3)–C(29), 50.6(4); C(28)–Co(3)–C(29), 38.9(6); C(28)–Co(4)–C(29), 39.2(6); Co(3)–Co(4)–C(28), 51.9(5); Co(3)–Co(4)–C(29), 50.0(5); Co(3)–C(28)–C(29), 67 (1); Co(4)–C(28)–C(29), 70.0(9); Co(3)–C(28)–C(22), 128(1); Co(4)–C(28)–C(22), 135(1); C(13)–C(14)–C(15), 142(1); C(22)–C(28)–C(29), 147(1); C(25)–C(30)–C(31), 129(1)°.

*4.2.1. [{$Co_2(CO)_6$}$_2$$Me_3SiC_2(C_{13}H_8)C_2SiMe_3$] (**1**)*

In a typical run, a solution of [$Co_2(CO)_8$] (0.19 g, 0.56 mmol) and 2,7-bis(trimethylsilylethynyl)fluorene (0.10 g, 0.28 mmol) in *n*-hexane (20 cm^3) was stirred at 0°C and the reaction progress was monitored by IR spectroscopy and spot TLC. After 1 h the solution turned dark brown and completion of the reaction was revealed from TLC and the disappearance of the bridging carbonyls due to [$Co_2(CO)_8$]. The solvent was then removed in vacuo and the residue was chromatographed on silica TLC plates using hexane as eluent. The major reddish–brown band was isolated to afford compound **1** as a dark-red microcrystalline solid in 51% yield (0.13 g) after recrystallization from a CH_2Cl_2–hexane mixture (Found: C, 45.02; H, 2.52. Calc. for $C_{35}H_{26}O_{12}Si_2Co_4$: C, 45.18; H, 2.82%).

*4.2.2. [{$Co_2(CO)_6$}$_2$$Me_3SiC_2(C_{13}H_6O)C_2SiMe_3$] (**2**)*

This complex was prepared using the conditions described for **1** but 2,7-bis(trimethylsilylethynyl)fluoren-9-one (0.10 g, 0.28 mmol) was used instead of 2,7-bis(trimethylsilylethynyl)fluorene. The major brown band was collected and compound **2** was obtained in 53% yield (0.14 g) (Found: C, 44.29; H, 2.43. Calc. for $C_{35}H_{24}O_{13}Si_2Co_4$: C, 44.51; H, 2.56%).

*4.2.3. [{$Co_2(CO)_6$}$_2$$Me_3SiC_2(C_4H_2S)_2C_2SiMe_3$] (**3**)*

This compound was prepared on a 0.28 mmol scale by the same method described for **1** and **2**. Preparative TLC purification eluting with hexane resulted in the isolation of **3** as a dark-red microcrystalline solid in 14% yield (0.036 g) (Found: C, 39.02; H, 2.40. Calc. for $C_{30}H_{22}O_{12}Si_2S_2Co_4$: C, 38.72; H, 2.38%).

*4.2.4. [{$Co_2(CO)_6$}$_2$$Me_3SiC_2(C_{14}H_7Fc)C_2SiMe_3$] (**4**)*

Similar procedures as for complex **1** were employed using [$Co_2(CO)_8$] (0.19 g, 0.56 mmol) and 9-ferrocenylmethylene-2,7-bis(trimethylsilylethynyl)fluorene (0.16 g, 0.28 mmol) to produce reddish–brown **4** in 49% yield (0.15 g) after TLC purification and recrystallization (Found: C, 48.92; H, 2.98. Calc. for $C_{46}H_{34}O_{12}Si_2Co_4Fe$: C, 49.05; H, 3.04%).

*4.2.5. [{$Co_2(CO)_6$}$_2$$HC_2(C_{13}H_8)C_2H$] (**5**)*

This compound was synthesized as described above for **1** from [$Co_2(CO)_8$] (0.19 g, 0.56 mmol) and 2,7-diethynylfluorene (0.06 g, 0.28 mmol) in *n*-hexane (20 cm^3). After the usual work-up, the crude product was purified by preparative TLC on silica eluting with hexane to yield dark-red product **5**. Recrystallization from CH_2Cl_2–hexane led to deep-red crystals of **5** in 54% yield (0.12 g) (Found: C, 43.99; H, 1.15. Calc. for $C_{29}H_{10}O_{12}Co_4$: C, 44.31; H, 1.28%).

*4.2.6. [{$Co_2(CO)_6$}$_2$$HC_2(C_{13}H_6O)C_2H$] (**6**)*

Compound **6** was prepared on a 0.28 mmol scale by the same synthetic methodology as for **1** using 2,7-diethynylfluoren-9-one (0.06 g, 0.28 mmol). TLC separation followed by recrystallization gave the desired product **6** as a major red solid in 55% yield (0.12 g) (Found: C, 43.22; H, 0.94. Calc. for $C_{29}H_8O_{13}Co_4$: C, 43.53; H, 1.01%).

*4.2.7. [{$Co_2(CO)_6$}$_2$$HC_2(C_4H_2S)_2C_2H$] (**7**)*

5,5′-Diethynyl-2,2′-bithiophene (0.06 g, 0.28 mmol) and [$Co_2(CO)_8$] (0.19 g, 0.56 mmol) were mixed in *n*-hexane (20 cm^3) at 0°C. The residue was worked-up, as before, to yield a dark-red crystalline solid (0.03 g, 15%) (Found: C, 36.52; H, 0.71. Calc. for $C_{24}H_6O_{12}S_2Co_4$: C, 36.67; H, 0.77%).

*4.2.8. [{$Co_2(CO)_6$}$_2$$HC_2(C_{14}H_7Fc)C_2H$] (**8**)*

This compound was made from [$Co_2(CO)_8$] (0.19 g, 0.56 mmol) together with 9-ferrocenylmethylene-2,7-diethynylfluorene (0.11 g, 0.28 mmol) following the same experimental procedures described above. The product **8** was isolated in 49% yield (0.13 g) (Found: C, 48.68; H, 1.69. Calc. for $C_{40}H_{18}O_{12}Co_4Fe$: C, 48.92; H, 1.85%).

4.3. Crystallography

Dark-red crystals of complexes **2**, **5**, **6**, **7** and **8** suitable for X-ray diffraction experiments were grown by slow evaporation of their respective solution in *n*-hexane–CH_2Cl_2 at r.t. Suitable crystals were glued on glass fibers with epoxy resins and intensity data were collected on a Mar Research Image Plate Scanner (**2**, **5**, **6** and **8**) or a Rigaku AFC7R diffractometer (**7**) equipped with graphite-monochromated Mo–K_α radiation ($\lambda = 0.71073$ Å). All pertinent crystallographic data and other experimental details are summarized in Table 3.

The space groups of each crystal were determined from the systematic absences and Laue symmetry check and confirmed by successful refinement of the structure. All possible alternatives $P\bar{4}2m$ and $P\bar{4}m2$ (for **6**) and *Cc* (for **8**) were tried but did not give any reasonable solution. The structures of **2**, **6** and **8** were solved by direct methods (SIR 92) [19] whereas those of **5** and **7** by Patterson methods (DIRDIF92 PATTY) [20]. The complete structure of each compound was subsequently established by Fourier-difference syntheses and refined on *F* by full-matrix least-squares analysis. In each case, hydrogen atoms were generated in their idealized positions (C–H 0.95 Å). All calculations were performed on Silicon-Graphics computer using the program package TEXSAN [21].

5. Supplementary material

Crystallographic data (comprising hydrogen atom coordinates, thermal parameters and full tables of bond

Table 3
Summary of crystal structure data for complexes **2**, **5**, **6**, **7** and **8**

	2	**5**	**6**	**7**	**8**
Empirical formula	$C_{35}H_{24}O_{13}Si_2Co_4$	$C_{29}H_{10}O_{12}Co_4$	$C_{29}H_8O_{13}Co_4$	$C_{24}H_6O_{12}S_2Co_4$	$C_{40}H_{18}O_{12}Co_4Fe$
Molecular weight	944.47	786.12	800.11	786.16	982.15
Crystal size (mm)	$0.13\times0.14\times0.21$	$0.25\times0.26\times0.29$	$0.24\times0.26\times0.29$	$0.26\times0.27\times0.31$	$0.24\times0.28\times0.31$
Crystal system	Orthorhombic	Triclinic	Tetragonal	Monoclinic	Monoclinic
Space group	*Pbca* (No. 61)	$P\bar{1}$ (No. 2)	$P\bar{4}$ (No. 81)	$P2_1$ (No. 4)	$C2/c$ (No. 15)
Unit cell dimensions					
a (Å)	16.793(1)	8.202(1)	16.485(1)	8.789(5)	45.517(1)
b (Å)	16.406(1)	12.029(1)	16.485(1)	18.748(8)	14.673(1)
c (Å)	29.917(2)	16.563(1)	11.450(1)	9.147(5)	11.735(1)
α (°)	90	104.79(1)	90	90	90
β (°)	90	92.20(1)	90	108.59(5)	90.26(1)
γ (°)	90	106.76(1)	90	90	90
V (Å^3)	8242.3(8)	1501.8(3)	3111.6(3)	1428(1)	7837.4(7)
$D_{calc.}$ (g cm^{-3})	1.522	1.738	1.708	1.828	1.665
Z	8	2	4	2	8
μ (Mo–K$_\alpha$) (cm^{-1})	16.99	22.34	21.61	24.90	20.82
$F(000)$	3792	776	1576	772	3904
$2\theta_{max}$ (°)	50.8	50.8	48.4	50.0	49.3
Reflections collected	52422	13097	28046	5580	30154
Unique reflections	4513	3891	2046	2614	3627
R_{int}	0.097	0.048	0.082	0.057	0.094
Observed reflections [$I>1.5\sigma(I)$]	2339	2498	1382	1534	1949
No. of parameters	312	406	270	253	314
Weighting scheme $w=[\sigma_c^2(F_o)+p^2/4F_o^2]^{-1}$	$p=0.021$	$p=0.020$	$p=0.023$	$p=0.018$	$p=0.024$
R [a]	0.066	0.044	0.046	0.077	0.072
R_w [b]	0.063	0.044	0.043	0.078	0.068
Goodness-of-fit	1.89	1.00	1.47	2.10	1.82
Residual extrema in final diff. map (e Å^{-3})	0.71 to −0.42	0.35 to −0.41	1.54 to −1.16	1.60 to −0.74	0.77 to −0.45

[a] $R=\Sigma||F_o|-|F_c||/\Sigma|F_o|$.
[b] $R_w=[\Sigma w(|F_o|-|F_c|)^2/\Sigma w(F_o)^2]^{1/2}$.

lengths and angles) for the structural analysis have been deposited with the Cambridge Crystallographic Centre (deposition nos. 132689–132693). Copies of this information may be obtained free of charge from The Director, CCDC, 12 Union Road, Cambridge, CB2 1EZ, UK (Fax: +44-1223-336033; e-mail: deposit@ccdc.cam.ac.uk or www: http://www.ccdc.cam.ac.uk).

Acknowledgements

We gratefully acknowledge the Hong Kong Baptist University for financial support.

References

[1] (a) G.J. Ashwell, D. Bloor (Eds.), Organic Materials for Nonlinear Optics III, Sec. Publ. No. 137, RSC, London, 1992. (b) J.L. Bredas, R.R. Chance (Eds.), Conjugated Polymer Materials: Opportunities in Electronic, Optoelectronic and Molecular Electronics, NATO ASI Series, vol. 182, Kluwer, Dordrecht, 1990. (c) J.E. Sheets, C.E. Carraher, Jr., C.U. Pittman, Jr. (Eds.), Metal-Containing Polymeric Systems, Plenum, New York, 1985.
[2] S. Patai (Ed.), The Chemistry of Carbon–Carbon Triple Bond, Wiley-Interscience, Chichester, UK, 1978.
[3] F. Diederich, Y. Rubin, Angew. Chem. Int. Ed. Engl. 31 (1992) 1101.
[4] Y. Rubin, C.B. Knobler, F. Diederich, J. Am. Chem. Soc. 112 (1990) 4966.
[5] M.M. Haley, B.L. Langsdorf, Chem. Commun. (Cambridge) (1997) 1121.
[6] (a) R.S. Dickson, P.J. Fraser, Adv. Organomet. Chem. 12 (1974) 323. (b) P.L. Pauson, Tetrahedron 41 (1985) 5855. (c) P. Magnus, D.P. Becker, J. Chem. Soc. Chem. Commun. (1985) 640. (d) N.M. Agh-Atabay, W.E. Lindsell, P.N. Preston, P.J. Tomb, A.D. Lloyd, R. Raugel-Rojo, G. Spruce, B.S. Wherrett, J. Mater. Chem. 2 (1992) 1241.
[7] W.E. Geiger, N.G. Connelly, Adv. Organomet. Chem. 24 (1985) 87.
[8] B.H. Robinson, J. Simpson, in: M. Chanon, M. Juillard, J.C. Poite (Eds.), Paramagnetic Organometallic Species in Activation/Selectivity, Catalysis, NATO ASI Series, vol. 257, Kluwer, Dordrecht, 1989.
[9] S.B. Colbran, B.H. Robinson, J. Simpson, J. Chem. Soc. Chem. Commun. (1982) 1362.

[10] (a) J.L. Davidson, in: P.S. Braterman (Ed.), Reactions of Coordinated Ligands, vol. 1, Plenum Press, New York, 1986, p. 825. (b) K.M. Nicholas, M.O. Nestle, D. Seyferth, in: H. Alper (Ed.), Transition Metal Organometallics in Organic Synthesis, vol. 2, Academic Press, New York, 1978, p. 2. (c) B.F.G. Johnson, J. Lewis, P.R. Raithby, D.A. Wilkinson, J. Organomet. Chem. 408 (1991) C9. (d) J. Lewis, B. Lin, M.S. Khan, M.R.A. Al-Mandhary, P.R. Raithby, J. Organomet. Chem. 484 (1994) 161.

[11] M. Arewgoda, P.H. Rieger, B.H. Robinson, J. Simpson, S.J. Visco, J. Am. Chem. Soc. 104 (1982) 5633.

[12] (a) T.J. Skotheim (Ed.), Handbook of Conducting Polymers, vols. 1 and 2, Marcel Dekker, New York, 1986. (b) F. Martinez, R. Voelkel, D. Naegele, H. Naarmann, Mol. Cryst. Liq. Cryst. 167 (1989) 227. (c) Z. Xu, D. Fichou, G. Horowitz, F. Garnier, Adv. Mater. 3 (1991) 150. (d) K. Yoshino, Synth. Met. 28 (1989) C669. (e) H.E. Katz, J. Mater. Chem. 7 (1997) 369. (f) J. Lewis, P.R. Raithby, W.Y. Wong, J. Organomet. Chem. 556 (1998) 219. (g) J. Lewis, N.J. Long, P.R. Raithby, G.P. Shields, W.Y. Wong, M. Younus, J. Chem. Soc. Dalton Trans. (1997) 4283. (h) W.Y. Wong, W.K. Wong, P.R. Raithby, J. Chem. Soc. Dalton Trans. (1998) 2761.

[13] C.E. Housecroft, B.F.G. Johnson, M.S. Khan, J. Lewis, P.R. Raithby, M.E. Robson, D.A. Wilkinson, J. Chem. Soc. Dalton Trans. (1992) 3171.

[14] (a) S. Aime, L. Milone, R. Rossetti, P.L. Stanghellini, Inorg. Chim. Acta 22 (1977) 135. (b) R.K. Harris, Nuclear Magnetic Resonance Spectroscopy: A Physiochemical View, Pitman, London, 1983.

[15] D. Osella, L. Milone, C. Nervi, M. Ravera, J. Organomet. Chem. 488 (1995) 1.

[16] (a) G.H. Worth, B.H. Robinson, J. Simpson, Organometallics 11 (1992) 3863. (b) G.H. Worth, B.H. Robinson, J. Simpson, J. Organomet. Chem. 387 (1990) 337.

[17] M.I. Bruce, B.D. Kelly, B.W. Skelton, A.H. White, J. Chem. Soc. Dalton Trans. (1999) 847.

[18] W.L.F. Armarego, D.D. Perrin, Purification of Laboratory Chemicals, fourth ed., Butterworth–Heinemann, London, 1996.

[19] A. Altomare, M. Cascarano, C. Giacovazzo, A. Guagliardi, J. Appl. Crystallogr. 26 (1993) 343.

[20] P.T. Beurskens, G. Admiraal, G. Beurskens, W.P. Bosman, S. Garcia-Granda, R.O. Gould, J.M.M. Smits, C. Smykalla, PATTY, The DIRDIF program system, Technical Report of the Crystallography Laboratory, University of Nijmegen, 1992.

[21] TEXSAN, Single-crystal Structure Analysis Software, Version 1.7, Molecular Structure Corporation, The Woodlands, TX, 1995.